

Uniformly Ergodic Data-Augmented MCMC for Fitting the General Stochastic Epidemic Model to Incidence Data

Raphaël Morsomme*

Department of Statistical Science, University of Duke

and

Jason Xu

Department of Statistical Science, University of Duke

January 13, 2022

Abstract

Stochastic epidemic models provide an interpretable probabilistic description of the spread of a disease through a population. Yet, fitting these models when the epidemic process is only partially observed is a notoriously difficult task due to the intractability of the likelihood for many classical models. To remedy this issue, this article introduces a novel data-augmented MCMC algorithm for fast and exact Bayesian inference for the stochastic SIR model given discretely observed infection incidence counts. In a Metropolis-Hastings step, new event times of the latent data are jointly proposed from a surrogate process that closely resembles the SIR, and from which we can efficiently generate epidemics compatible with the observed data.

The proposed DA-MCMC algorithm is fast and, since the latent data are generated from a faithful approximation of the target model, a large portion thereof can be updated per iteration without prohibitively lowering the acceptance rate. We find that the method explores the high-dimensional latent space efficiently and scales to outbreaks with hundreds of thousands of individuals, and we show that the Markov chain underlying the algorithm is uniformly ergodic. We validate its performance via thorough simulation experiments and a case study on the 2013-2015 Ebola outbreak in Western Africa.

Keywords: Stochastic epidemic model; incidence data; exact Bayesian inference; likelihood-based inference

*The authors gratefully acknowledge *please remember to list all relevant funding sources in the unblinded version*

1 Introduction

The efficient control of a disease outbreak requires an understanding of the mechanisms underlying its spread. Mechanistic compartmental models, which describe the transition of individuals between various states, have a long mathematical modeling tradition in epidemiology dating back to (15). Due to their interpretability, they are commonly used to describe the dynamics of an outbreak and typically serve as the main source of information for predicting the course of an outbreak and identifying interventions that could be effective. Originally, deterministic versions of the models were employed by mathematicians and epidemiologists. These models are simple to analyze, but fail to capture the inherent randomness characterizing the spread of a disease. For instance, they cannot be used to estimate the probability of a large-scale outbreak or its expected duration, and do not allow for uncertainty quantification when used within inferential procedures. Stochastic epidemic models (SEM), on the other hand, incorporate the random nature of infections and recoveries and therefore provide more realistic descriptions of the spread of a disease, and in turn more reliable inference from observed data.

Conducting inference on SEMs is, however, a notably difficult task. Challenges stem from the fact that the observed data typically provide incomplete information on a process that evolves continuously through time, making the likelihood of the model intractable. In practice, one often has access to either incidence data such as weekly counts of new infections, or prevalence data such as the numbers of infectious individuals at discrete reporting times. The marginal likelihood of such partially observed data becomes a computational bottleneck, as it requires a large integration step that accounts for all possible configurations of the missing epidemic process. In particular, direct computation of this likelihood requires the transition probabilities between observation times for which no closed form is

available. Moreover, given the size of the transition matrix, classical matrix exponentiation is intractable. Numerical methods to obtain transition probabilities have recently been developed in (11), but the high computational costs limit their approach to moderate sized outbreaks.

In this article, we employ data augmentation to explore configurations of the missing data through latent variables. We introduce a uniformly ergodic data-augmented MCMC (DA-MCMC) algorithm that targets the exact joint posterior of model parameters and these latent variables under the stochastic SIR model, a commonly used SEM, from discretely observed incidence counts of infections. Rather than marginalizing directly, our approach accounts for the latent space via sampling. The algorithm updates the event times of the augmented data by jointly proposing infection and removal times from a surrogate stochastic process whose dynamics closely resemble those of the SIR process, and from which we can efficiently generate an epidemic that is compatible with the observed data. Its success lies in the design of this surrogate process serving as an efficient proposal scheme within a Metropolis-Hastings algorithm. Since the latent spaces are generated from a faithful approximation of the target epidemic model, the algorithm can update a large portion of the event times per iteration while maintaining a high acceptance rate, thereby exploring the high-dimensional latent space efficiently. Our approach is fully Bayesian and therefore allows representation of parameter uncertainty through posterior distributions.

The remainder of the article is structured as follows. Section 2 provides background information on the inference task. It introduces the stochastic SIR model and explains why conducting inference from partially observed data is a difficult task. Previous works addressing this problem are also presented. Section 3.1 introduces the DA-MCMC algorithm and describes the surrogate process from which the latent data are generated in the

Metropolis-Hastings step. The similarity between the surrogate and the target processes is assessed in Section 3.2 and the DA-MCMC is shown to be uniformly ergodic in Section 3.3. In Section 4.1, we examine the performance of our algorithm on simulated data and then turn to an analysis of the 2013-2015 Ebola outbreak in Guéckédou, Guinea, in Section 4.2. Finally, Section 5 discusses the findings and concludes the article.

2 Background and Prior Work

2.1 The Stochastic SIR Model

Our point of departure is to consider the stochastic SIR model introduced by (?) – also referred to as the general stochastic epidemic model – which offers a parsimonious and interpretable representation of the mechanistic dynamics of an epidemic. The stochastic SIR model is a compartmental model in which individuals transition through three states or compartments: susceptible (S), infectious (I) and removed (R). The only possible moves are from S to I (infections) and from I to R (removals). A susceptible individual becomes infected through contact with an infectious individual. Once infected, she is immediately infectious and remains so for some period of time after which she is removed from the process without the possibility of reinfection. In this formulation, demographic dynamics such as births and deaths are ignored since they usually occur at a much slower rate than infections and removals.

Assuming a closed population of size n , the stochastic SIR model consists of a continuous-time vector-valued process

$$\mathbf{X} = \{\mathbf{X}(t), t > 0\} \in \chi_{\mathbf{X}} \quad (1)$$

with

$$\mathbf{X}(t) = (X_1(t), \dots, X_n(t)) \in \{s, i, r\}^n \quad (2)$$

where the agent-level subprocess

$$X_j(t) = \begin{cases} s, & t \in [0, \tau_j^I] \\ i, & t \in (\tau_j^I, \tau_j^R], \quad i = 0, \dots, n \\ r, & t \in (\tau_j^R, \infty) \end{cases}$$

denotes the compartment of individual j at time t with τ_j^I and τ_j^R respectively the infection and removal times of individual j . If individual j never becomes infectious, we set $\tau_j^I = \tau_j^R = \infty$ and $X_j(t) = s$ for $t \in [0, \infty)$. Since removed individuals do not contribute to the pandemic, it is safe to ignore the individuals removed at time 0 and write $n = S(0) + I(0)$. Here the space $\chi_{\mathbf{X}}$ denotes the set of trajectories compatible with the evolution of a disease—that is, the set of trajectories in which no infection occurs when the infectious compartment is depleted:

$$\chi_{\mathbf{X}} = \{\mathbf{X} : \mathbf{X}(t) \in \{s, r\}^n \Rightarrow \mathbf{X}(t+u) = \mathbf{X}(t), \forall u > 0\}. \quad (3)$$

The stochastic SIR model is specified by the rates at which individuals move from one compartment to another. If we assume a homogeneously mixing population where contacts between individuals occur independently at some constant rate β , the contacts between two given individuals are said to follow a Poisson process with rate β . This parameter can be interpreted as the *infection rate*: when a susceptible individual comes into contact with an infectious individual, she immediately becomes infectious. If we also make the common assumption that the infectious periods follow independent exponential distributions with rate γ , then the process (1) is a time-homogeneous continuous time Markov chain, whose

instantaneous transition rates are given by the matrix $\Lambda = [\lambda_{\mathbf{x}, \mathbf{x}'}]$ with

$$\lambda_{\mathbf{x}, \mathbf{x}'} = \begin{cases} \beta I(t), & \mathbf{x} \text{ and } \mathbf{x}' \text{ only differ at position } j \text{ with } x_j = s \text{ and } x'_j = i, \\ \gamma, & \mathbf{x} \text{ and } \mathbf{x}' \text{ only differ at position } j \text{ with } x_j = i \text{ and } x'_j = r, \\ 0, & \text{otherwise.} \end{cases} \quad (4)$$

where $I(t) = \#\{x_j(t) = i\}$ is the total number of infectious individuals at time t . Thus, the individual-level infection and removal rates at time t are respectively $\beta I(t)$ and γ .

2.2 Inference with Complete Data

When the Markov process (1) is completely observed until time t_{end} , we obtain the following likelihood (?)

$$\begin{aligned} L(\theta; \mathbf{X}) &= \prod_{j \in \mathcal{I}} \beta I(\tau_j^I) \prod_{k \in \mathcal{R}} \gamma \exp \left\{ - \int_0^{t_{end}} \beta S(t) I(t) + \gamma I(t) dt \right\} \\ &= \beta^{n_I} \gamma^{n_R} \prod_{j \in \mathcal{I}} I(\tau_j^I) \exp \left\{ -\beta \int_0^{t_{end}} S(t) I(t) - \gamma \int_0^{t_{end}} I(t) dt \right\} \end{aligned} \quad (5)$$

describing the complete data trajectory. To establish notation, $\theta = (\beta, \gamma) \in \chi_\theta$ are the model parameters and $\chi_\theta = (0, \infty) \times (0, \infty)$ denotes the parameter space, the index sets $\mathcal{I} = \{j : \tau_j^I \in (0, t_{end}]\}$ and $\mathcal{R} = \{j : \tau_j^R \in (0, t_{end}]\}$ denote the individuals that are respectively infected and removed during the observation interval $(0, t_{end}]$, $n_I = |\mathcal{I}|$ and $n_R = |\mathcal{R}|$ are the numbers of observed infections and removals, and $S(t) = \#\{X_i(t) = s\}$ is the number of susceptible individuals at time t .

It is straightforward to conduct inference in this continuously observed scenario . The likelihood (5) belongs to the exponential family, and maximum likelihood estimates of its parameters can be expressed in terms of the sufficient statistics defined above as

$$\hat{\beta} = \frac{n_I}{\int_0^{t_{end}} S(t) I(t) dt}, \quad \hat{\gamma} = \frac{n_R}{\int_0^{t_{end}} I(t) dt}.$$

Note that since the functions $I(t)$ and $S(t)$ are constant between event times, the two integrals correspond to finite sums which are straightforward to compute. Furthermore, in a Bayesian context, inference is facilitated by the conjugacy of (5) with the gamma distribution. If we use independent gamma priors

$$\beta \sim G(a_\beta, b_\beta), \quad \gamma \sim G(a_\gamma, b_\gamma) \quad (6)$$

where $G(a, b)$ denotes the parametrization of the gamma distribution with mean a/b and variance a/b^2 , we obtain the independent posterior distributions

$$\beta|\mathbf{X} \sim G\left(a_\beta + n_I, b_\beta + \int_0^{t_{end}} I(t)S(t)dt\right) \quad (7)$$

$$\gamma|\mathbf{X} \sim G\left(a_\gamma + n_R, b_\gamma + \int_0^{t_{end}} I(t)dt\right) \quad (8)$$

from which one can easily generate independent values to explore the distribution $\pi(\theta|\mathbf{X})$ via Monte Carlo.

The likelihood (5) can also be parameterized in terms of $\tilde{\theta} = (\beta, R_0)$ where $R_0 := S(0)\beta/\gamma$ is called the basic reproduction number and corresponds to the expected number of secondary infections caused by an infectious individual in a susceptible population. Using $\tilde{\theta}$ with the independent prior distributions

$$\beta \sim G(a_\beta, b_\beta), \quad R_0 \sim IG(a_R, b_R), \quad (9)$$

where IG denote the inverse-gamma distribution, yields the closed-form full conditional distributions.

$$\beta|\mathbf{X}, R_0 \sim G\left(a_\beta + n_I + n_R, b_\beta + \int_0^{t_{end}} S(t)I(t)dt + \frac{S(0)}{R_0} \int_0^{t_{end}} I(t)dt\right) \quad (10)$$

$$R_0|\mathbf{X}, \beta \sim IG\left(a_R + n_R, b_R + \beta S(0) \int_0^{t_{end}} I(t)dt\right) \quad (11)$$

We have observed that the parameterization $\tilde{\theta}$ results in a Markov chain that mixes better and therefore employ it in the simulation studies and data analysis of Section 4.

2.3 Inference with Incomplete Data

In practice, inference is complicated by the fact that the epidemic process (1) is only partially observed. When some event times are unobserved, we do not have access to the sufficient statistics needed to evaluate the likelihood (5). Various types of partially observed data typify real data and have been considered in the literature. These include the removal times in (8) and (20) or the number of infectious individuals at discrete points in time in (5). For instance, the former arises in animal experiments in which positive cases are immediately isolated from the rest of the population and no longer contribute to disease spread. In such cases, exact times of removals are known, but this information is unavailable in a typical observational study.

In this article, we focus our attention on partial data consisting of *incidence* counts of infections during given time intervals, e.g. weekly infection counts. Such data arise when an infectious individual is identified some time after onset and may continue to infect others after being tested positive for the disease. Given an observation schedule $t_{0:K}$ ($K \geq 1$) with $0 = t_0 < t_1 < \dots < t_K = t_{end}$, the observed data consist of the K -dimensional vector $\mathbf{Y} = I_{1:K}$ where $I_k = \#\{\tau_j^I \in (t_{k-1}, t_k]\}$ is the number of infections during the k^{th} interval.

This form of observed data is motivated by the 2013-2015 outbreak of the Ebola virus, the largest outbreak since the discovery of the virus in 1976, which resulted in at least 11,000 deaths, the majority of which occurred in three Western African countries (Guinea, Liberia and Sierra Leone). The data available for this outbreak consist of weekly number of positive tests. This outbreak was characterized by the large number of infections that occurred after individuals were tested positive for the virus, giving rise to noisy incidence data. (?) reports that numerous infections took place at the hospitals where infected

individuals received treatment as well as at the funerals of people deceased from the virus¹.

We therefore model the weekly number of positive tests as the weekly number of infections in a SIR model.

In a Bayesian framework, the posterior distribution of the parameters given the observed data is formally related to the complete data likelihood (5) via integration:

$$\pi(\theta|\mathbf{Y}) \propto \pi(\theta)L(\theta; \mathbf{Y}) = \pi(\theta) \int_{\chi_{\mathbf{x}}} L(\theta; \mathbf{x})\delta_{\mathbf{Y}}(\mathbf{x})d\mathbf{x} \quad (12)$$

where $\pi(\theta)$ is the prior distribution on θ , and $\delta_{\mathbf{Y}}(\mathbf{x}) = 1$ if \mathbf{x} is compatible with the observed infection counts \mathbf{Y} and 0 otherwise; that is, the partial data likelihood $L(\theta; \mathbf{Y})$ consists of a high-dimensional integral over all epidemic paths that agree with the observed data. This marginalization step has no known closed-form solution and presents computational challenges even for a population of moderate size.

2.4 Prior Work

Researchers have explored several approaches for conducting inference on partially observed stochastic epidemic processes. Early approaches include the use of martingale-based equations (3; 26). However, such methods are difficult to apply to dynamic models with partially observed data and are therefore not suitable to the stochastic SIR model with incomplete data. More recently, researchers have based their computation on a simpler process that approximates the model's dynamics and whose likelihood in the presence of partially observed data is tractable. Popular approximations include chain binomial models (10; 1), diffusion processes (4; 6) and Gaussian processes (14). While these approximation-based

¹In most regions impacted by the Ebola virus, touching the body of the deceased during funerals is a tradition. Since the Ebola virus is transmitted via bodily fluids such as sweat, numerous infections occurred at funerals.

approaches bypass the intractability of the partial data likelihood (12), the assumptions on which they are based are questionable when the population is small, and, as a result, the dynamic of the stochastic process differs from its asymptotic behavior.

Since the popularization of Markov chain Monte Carlo (MCMC) methods in statistics by (7) and (25), researchers have developed sampling-based methods to directly work with the SIR likelihood instead of an approximation thereof. MCMC algorithms fall into two categories: model-based forward simulation and data-augmented MCMC (DA-MCMC). Particle filtering in (16) is an example of the former category that is popular among practitioners. Its plug-and-play feature makes it applicable to a wide variety of models. However, model-based forward simulation suffers from two drawbacks: simulating data from a model as complex as the SIR that is compatible with the observed data is prohibitively slow, and these methods can fail to converge when the model does not fit the data well. The approximate Bayesian computation (ABC) framework in (17) offers a solution to the latter problem, but its inference is based on an approximation of the model's likelihood. As a result, the inference can be biased, and it is difficult to evaluate the degree of approximation involved.

The second family of MCMC-based inferential methods treats the unobserved event times as nuisance parameters; that is, the observed data are augmented with latent variables that consist of the times and types of unobserved epidemic events. Researchers have mostly focused on the development of more efficient proposal schemes to explore this high-dimensional latent space. (8) and (20) employed the reversible-jump MCMC framework introduced by (9) to explore models with different numbers of unobserved events. These authors augment the observed data which consist of the recovery times with the unobserved infection times and explore the latent space by uniformly inserting, deleting or moving

an element of the latent data per iteration of the MCMC algorithm. More recently, (?)) proposed a sampler for epidemics over networks when the infection times are assumed to be known, and (5) designed a sampler to conduct inference with discretely observed prevalence counts, with latent data consisting of the infection and recovery times of each individual. Their algorithms explore the latent spaces by updating the event times of a single individual per iteration of the MCMC algorithm. In the discrete-time setting, (?) constructed a Gibbs sampler to update the trajectory of an individual per iteration. These DA-MCMC methods suffer from poor mixing in the presence of large epidemics. Since they update a very small number of latent variables per iteration, the resulting Markov chains is sticky: it makes very small jumps in the latent space and therefore requires a large number of iterations to explore it completely. Although the update of a slightly larger number of event times per iteration in (21) and the non-centered parameterization of (18) may improve the performance of the algorithms, the gains are modest; the Markov chains still suffer from a high level of auto-correlation and do not possess satisfactory mixing properties in populations over a few hundred individuals. By a slight abuse of language, we will refer to these DA-MCMC algorithms as *single-site-update* (SSU) DA-MCMC algorithms to contrast them to the method proposed in this article in which the entire latent data are jointly updated.

3 Exact Inference with a Data-Augmented Approach

We adopt a data-augmented MCMC approach that bridges the challenging partially observed setting to the tractable complete data likelihood by way of latent variables. Our method hinges on the efficacy of a carefully designed proposal process for the latent variables that faithfully approximates the SIR process dynamics. The Metropolis-Hastings

sampler for the latent data targets the exact posterior distribution under the SIR model given partially observed incidence data, and enjoys the efficiency of fast proposals in the high-dimensional latent space as well as fast computations involving the complete data likelihood.

As shown in Section 2.2, the complete data likelihood (5) is amenable to computation. This suggests augmenting the observed data \mathbf{Y} with latent data \mathbf{Z} such that the likelihood $L(\theta; (\mathbf{Y}, \mathbf{Z}))$ has the closed form (5), and constructing an ergodic Markov chain $\{(\theta^{(m)}, \mathbf{Z}^{(m)})\}_{m=0}^M$ on $\chi = \chi_\theta \times \chi_{\mathbf{z}}$ whose limiting distribution is the joint posterior $\pi(\theta, \mathbf{X}|\mathbf{Y})$. Given the draws $\{(\theta^{(m)}, \mathbf{Z}^{(m)})\}_{m=0}^M$, the sequence $\{\theta^{(m)}\}_{m=0}^M$ provides an approximation of the marginal posterior distribution of interest $\pi(\theta|\mathbf{Y})$.

We consider the latent data $\mathbf{Z} = \{(z_j^I, z_j^R)\}_{j=1}^n$ which consist of the times of the two types of unobserved epidemic events, where the infection and removal times of individual j are respectively

$$z_j^I \begin{cases} \in [0, t_{end}) & \text{if individual } j \text{ is infected before } t_{end} \\ = \infty & \text{if individual } j \text{ is not infected before } t_{end} \end{cases}$$

and

$$z_j^R \begin{cases} \in (z_j^I, t_{end}] & \text{if individual } j \text{ is removed before } t_{end} \\ = \infty & \text{if } z_j^I = \infty \text{ or individual } j \text{ is not removed before } t_{end}. \end{cases}$$

Since $\mathbf{Y} = I_{1:K}$ is a deterministic function of the infection events, the joint posterior distribution is

$$\pi(\theta, \mathbf{Z}|\mathbf{Y}) \propto \delta_{\mathbf{Y}}(\mathbf{Z}) L(\theta; \mathbf{Z}) \pi(\theta)$$

where $L(\theta; \mathbf{Z})$ is the complete data likelihood (5).

We construct a DA-MCMC algorithm that alternates between updates of the parameters θ given the current configuration of the latent data \mathbf{Z} , and updates of the latent data

given the current values of the parameters. A one-step transition from $\mathbf{x}_1 = (\theta_1, \mathbf{z}_1)$ to $\mathbf{x}_2 = (\theta_2, \mathbf{z}_2)$ therefore looks like

$$\mathbf{x}_1 = (\theta_1, \mathbf{z}_1) \rightarrow (\theta_2, \mathbf{z}_1) \rightarrow (\theta_2, \mathbf{z}_2) = \mathbf{x}_2.$$

The first update for θ is straightforward due to the Gamma conjugacy of the complete-data likelihood (5). We can simply draw from the two full conditional distributions (7). In these expressions, the sufficient statistics from \mathbf{Z} , $n_I, n_R, \int S(t)I(t)dt, \int I(t)dt$ are easy to compute. The second update for \mathbf{Z} , on the other hand, is difficult. Though unrestricted forward simulation of the stochastic SIR process is straightforward (?), drawing trajectories conditionally on the observed data amounts to *conditional* simulation of a Markov process, a notoriously difficult task (13). Since given the $\mathbf{Y} = I_{1:K}$ the end-point of the process are not known, the methods proposed in (13) are not immediately applicable. Instead, we generate the latent data conditionally on \mathbf{Y} from a surrogate process, and accept or reject them in a Metropolis-Hastings (MH) step. Given some current θ and \mathbf{z} , the MH step proceeds by simulating a candidate \mathbf{z}^* from a surrogate process $Q(\cdot|\theta)$ with density $q(\cdot|\theta)$, which we present in Section 3.1. Then \mathbf{z}^* is accepted with probability

$$\alpha((\theta, \mathbf{z}), (\theta, \mathbf{z}^*)) = \min \left\{ 1, \frac{L(\theta; \mathbf{z}^*) q(\mathbf{z}|\theta)}{L(\theta; \mathbf{z}) q(\mathbf{z}^*|\theta)} \right\}, \quad (13)$$

and otherwise the current \mathbf{z} is retained. Note that it is not necessary to compute $\delta_{\mathbf{Y}}(\mathbf{z})$ in the MH acceptance ratio (13) since \mathbf{z}^* is compatible with \mathbf{Y} by construction. Algorithm 1 provides the details of the DA-MCMC algorithm.

3.1 Efficient Proposal Process for Latent Data

The surrogate process that we consider for generating the latent data in the MH step consists of a stochastic process whose dynamics closely resemble those of the SIR and which

Algorithm 1 Data-Augmented MCMC Sampler

Require: $\theta^{(0)}$

return $\{(\mathbf{z}^{(m)}, \theta^{(m)})\}_{m=0}^N$

$\mathbf{z}^{(0)} \sim Q(\cdot | \theta^{(0)})$ (generate the initial latent data from the PD-SIR process)

for $j = 1, \dots, N$ **do**

$\beta^{(j)} | \mathbf{z}^{(j-1)} \sim Ga\left(a_\beta + n_I^{(j-1)}, b_\beta + \int_0^{t_{end}} I^{(j-1)}(t)S^{(j-1)}(t)dt\right)$ (Gibbs update)

$\gamma^{(j)} | \mathbf{z}^{(j-1)} \sim Ga\left(a_\gamma + n_R^{(j-1)}, b_\gamma + \int_0^{t_{end}} I^{(j-1)}(t)dt\right)$ (Gibbs update)

$\theta^{(j)} \leftarrow (\beta^{(j)}, \gamma^{(j)})$

$\mathbf{z}^* \sim Q(\cdot | \theta^{(j)})$ (generate latent data from the PD-SIR process)

$\alpha = \min \left\{ 1, \frac{L(\theta^{(j)}; \mathbf{z}^*) q(\mathbf{z}^{(j-1)} | \theta^{(j)})}{L(\theta^{(j)}; \mathbf{z}^{(j-1)}) q(\mathbf{z}^* | \theta^{(j)})} \right\}$

$u \sim U(0, 1)$

if $u < \alpha$ **then**

$\mathbf{z}^{(j)} \leftarrow \mathbf{z}^*$

else

$\mathbf{z}^{(j)} \leftarrow \mathbf{z}^{(j-1)}$

end if

end for

is designed for efficient simulation of epidemic trajectories compatible with the incidence data $\mathbf{Y} = I_{1:K}$. We refer to this surrogate process as the *piecewise decoupled SIR* process (PD-SIR). Similarly to the SIR, the PD-SIR process corresponds to a compartmental model in which individuals move from the compartments S to I and from I to R . The removal dynamics are identical under both processes: infectious periods follow independent exponential distributions with rate γ .

The infection dynamics, however, differ slightly. In the SIR process, the individual-level infection rate at time t is $\mu(t) = \beta I(t)$; see Equation (4). Note that μ varies after every event since the value of I changes after an infection or a removal. In contrast, in the PD-SIR process, the infection rate is kept constant over small periods of time. Consider the observation schedule of \mathbf{Y} , $t_{0:K}$. For $t \in (t_{k-1}, t_k]$, the infection rate of the PD-SIR process is defined as

$$\tilde{\mu}(t) := \beta I(t_{k-1}) = \mu_k$$

where $I(t_{k-1})$ denotes the number of infectious individuals at the beginning of the k th interval. As shown in Figure 1, the infection rate $\tilde{\mu}$ and the variable I are decoupled in each interval, and the infection rate is reset at the beginning of the intervals. Over a single interval, the PD-SIR process is equivalent to a recent two-type branching process approximation of the SIR dynamics proposed in (12).

It now becomes straightforward to simulate realizations from the PD-SIR process conditionally on the observations $\mathbf{Y} = I_{1:K}$. By construction, under the PD-SIR model the variable $S(t)$ follows a linear death process (LDP) during each interval with death rate $\mu_k = \beta I(t_{k-1})$. The LDP is a counting process possessing the so-called order statistics property (19); that is, given the number of events registered on some interval, the event times are distributed as the order statistics of independent and identically distributed (i.i.d.)

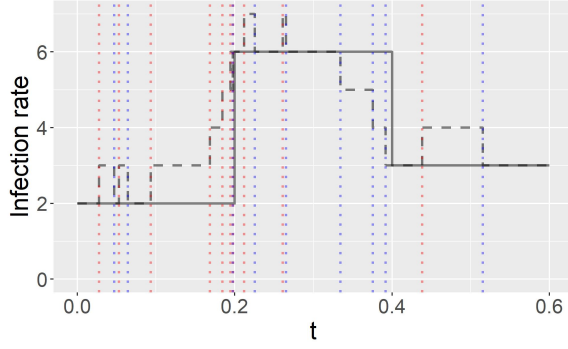


Figure 1: Infection dynamics of the SIR (dashed line) and PD-SIR (solid line) processes in a small population $((S(0), I(0)) = (10, 2))$ with $\beta = 1$. The schedule of the PD-SIR is $t_{0:3} = (0, 0.2, 0.4, 0.6)$. Vertical dotted lines indicate infection (red) and removal (blue) times.

random variables following, in the case of the LDP, a exponential distribution truncated to that interval.

Theorem 3.1. *Consider a linear death process with death rate μ and let $\tau_{1:N} \in (t_l, t_u]$ be the times of the N deaths occurring between times t_l and t_u . Then*

$$\tau_j \stackrel{d}{=} X_{(j)}, \quad j = 1, \dots, N$$

where $X_{(j)}$ is the j^{th} order statistics of N i.i.d. random variables following a truncated exponential distribution with rate μ , lower bound t_l and upper bound t_u .

Appendix A contains the proof of this theorem. Generating values from a truncated exponential distribution can be done extremely efficiently via the inverse cumulative distribution function method.

We can use Theorem 3.1 to generate latent data $\mathbf{z} = \{(z_i^I, z_i^R)\}_{i=1}^n$ compatible with $\mathbf{Y} = I_{1:K}$ from the PD-SIR process as follows. For each time interval $[t_{k-1}, t_k)$, we compute $\mu_k = \beta I(t_{k-1})$ and $U_k = I(0) + \sum_{l=1}^{k-1} I_l$, the cumulative number of infections that happened

before t_{k-1} . The index set $\mathcal{I}_k = \{U_k + 1, \dots, U_k + I_k\}$ therefore denotes the I_k individuals infected during the k th interval. Note that $I(t_{k-1})$ only depends on past events and can therefore be computed given the PD-SIR process up to time t_{k-1} . Algorithm 2 provides a simple recursion to compute this variable efficiently. For $j \in \mathcal{I}_k$, following Theorem 3.1, we sample the infection times $z_j^I \sim \text{TrunExp}(\mu_k; t_{k-1}, t_k)$, a truncated exponential distribution with rate μ_k bounded between t_{k-1} and t_k . For the same indices j , we then generate the removal times z_j^R from the removal dynamics of the SIR. To accomplish this, we sample the removal time of individual j from the mixed distribution

$$z_j^R | z_j^I \sim (1 - p_j) \delta_\infty + p_j \text{TrunExp}(\gamma; z_j^I, t_{end})$$

placing point mass $(1 - p_j)$ at ∞ and continuous mass on the interval $(z_j^I, t_{end}]$, where δ_∞ corresponds to the Dirac distribution with mass 1 on the element ∞ , and

$$p_j = 1 - \exp\{-\gamma(t_{end} - z_j^I)\} = P(z_j^R \leq t_{end} | z_j^I)$$

is the cumulative distribution function of an exponential distribution with rate γ .

By construction, this scheme generates latent data from the PD-SIR process that are compatible with $\mathbf{Y} = I_{1:K}$. The density q of the proposal kernel Q for the PD-SIR process corresponds to

$$\begin{aligned} q(\mathbf{z} | \theta) &= \prod_{k=1}^K \prod_{j \in \mathcal{I}_k} \text{TrunExp}(z_j^I; \mu_k, t_{k-1}, t_k) \\ &\quad \times \prod_{i=1}^n (1 - p_i)^{\mathbf{1}(z_i^R = \infty)} (p_i \text{TrunExp}(z_i^R; \gamma, z_i^I, t_{end}))^{\mathbf{1}(z_i^R \leq t_{end})} \end{aligned} \tag{14}$$

where

$$\text{TrunExp}(x; \mu, l, u) = \frac{\mu \exp\{-\mu x\}}{\exp\{-\mu l\} - \exp\{-\mu u\}}, \quad x \in (l, u)$$

denotes the density of a truncated exponential distribution with parameters as notated previously. Algorithm 2 provides a summary of the proposal scheme used to generate \mathbf{z}^* from Algorithm 1.

Algorithm 2 Generating a PD-SIR process conditionally on the observed data $\mathbf{Y} = I_{1:K}$

Require: $I_{1:K}, \theta = (\beta, \gamma), I(0)$

for $j = 1, \dots, I(0)$ **do**

$z_j^I \leftarrow 0$ (by the memoryless property of the exponential distribution).

$p_j \leftarrow 1 - \exp\{-\gamma(t_{end} - 0)\}$

$z_j^R \sim (1 - p_j)\delta_\infty + p_j \text{TrunExp}(\gamma, 0, t_{end})$

end for

for $k = 1, \dots, K$ **do**

$U_k \leftarrow I(0) + \sum_{l=1}^{k-1} I_l$

$\mathcal{I}_k \leftarrow \{U_k + 1, \dots, U_k + I_k\}$

$\mu_k \leftarrow \beta I(t_{k-1})$

$X_{\mathcal{I}_k} \sim \text{TrunExp}(\mu_k, t_{k-1}, t_k)$ i.i.d.

for $j \in \mathcal{I}_k$ **do**

$z_j^I \leftarrow X_{(j)}$ (infection times)

$p_j \leftarrow 1 - \exp\{-\gamma(t_{end} - z_j^I)\}$

$z_j^R \sim (1 - p_j)\delta_\infty + p_j \text{TrunExp}(\gamma, z_j^I, t_{end})$ (removal times)

end for

$R_k \leftarrow \#\{i : \tau_i^R \in (t_{k-1}, t_k]\}$ (number of removals in the k^{th} interval)

$I(t_k) \leftarrow I(t_{k-1}) + I_k - R_k$

end for

The following four characteristics of our DA-MCMC algorithm are worth noting. First, initializing the Markov chain only requires values for the initial parameters $\theta^{(0)} = (\beta^{(0)}, \gamma^{(0)})$ since $\mathbf{Z}^{(0)}$ can be generated conditionally on \mathbf{Y} and $\theta^{(0)}$ alone from the PD-SIR process. Second, since the PD-SIR closely approximates the SIR model, the acceptance rate in the MH step for the latent data is typically high. For large populations, however, the acceptance rate may drop considerably, thereby hindering the mixing of the Markov chain. To address this issue, we introduce a tuning parameter $\rho \in (0, 1]$ which determines the proportion of individuals whose trajectory is updated per iteration. That is, in a given MH step, we only update the infection and removal times of a subset of $\lceil \rho n \rceil$ individuals chosen uniformly at random. Smaller values for ρ result in smaller jumps in the latent space and a larger MH acceptance rate, which may lead to better overall mixing in large populations. Third, if all event times are updated ($\rho = 1$), then the proposed and current latent data are independent conditionally on the current values of the parameters: $\mathbf{Z}^{(k-1)} \perp \mathbf{Z}^* | \theta^{(k)}$. Our proposal scheme can therefore be said to be semi-independent, a characteristic that is crucial for proving the uniform ergodicity of the resulting Markov chain in Section 3.3. This contrasts with existing DA-MCMC algorithms which only update a small fraction of the latent data per iteration and generate consecutive configurations of the latent data that are mostly identical. Moreover, since the dimension of the latent data remains constant across iterations in our approach, we do not need to rely on reversible jump MCMC unlike (8) and (20). Finally, not only is proposing latent data from the PD-SIR process extremely fast since all the necessary random variables can be generated with the inverse cumulative distribution function method, but ensuring that the proposed latent data are compatible with the observed data is accomplished at no additional cost, making the proposal scalable to large outbreaks.

3.2 Quality of Approximation

In the special case $\rho = 1$, the latent data proposal is independent of the current configuration of the latent data. The efficiency of the DA-MCMC algorithm to explore the latent space is therefore directly related to the acceptance rate of the MH step, which in turn depends on how faithfully the surrogate process resembles the target process. If the two processes are similar, then the proposed latent data will often be accepted and the Markov chain will have better mixing properties.

The PD-SIR process only differs from the SIR process in its infection dynamics, with the removal dynamics being identical in the two processes. Figure 2 compares the trajectories of the compartments S , I and R of a SIR process of moderate size $((S(0), I(0)) = (1000, 10)$ with $(\beta, \gamma) = (0.003, 1)$ and $t_{end} = 6$) and those of four PD-SIR processes constrained to be compatible with the observed incidence data $I_{1:K}$ from the SIR process for $K \in \{5, 10, 50, 1000\}$. We see that the PD-SIR is qualitatively close to the SIR, even for small values of K . Unsurprisingly, the quality of the approximation improves as K increases. The seemingly piece-wise linear trajectory of the S compartment in the PD-SIR visible for small K comes from it following a LDP with piece-wise constant death rate. In the limit as $K \rightarrow \infty$, the infection times are effectively known under the PD-SIR and the two processes become equivalent. This observation that the PD-SIR faithfully approximates the SIR, even for moderate K , provides intuition for why our method can yield a high acceptance rate in the MH step. As a result, the algorithm can make large jumps in the high-dimensional latent space and thus explores it efficiently.

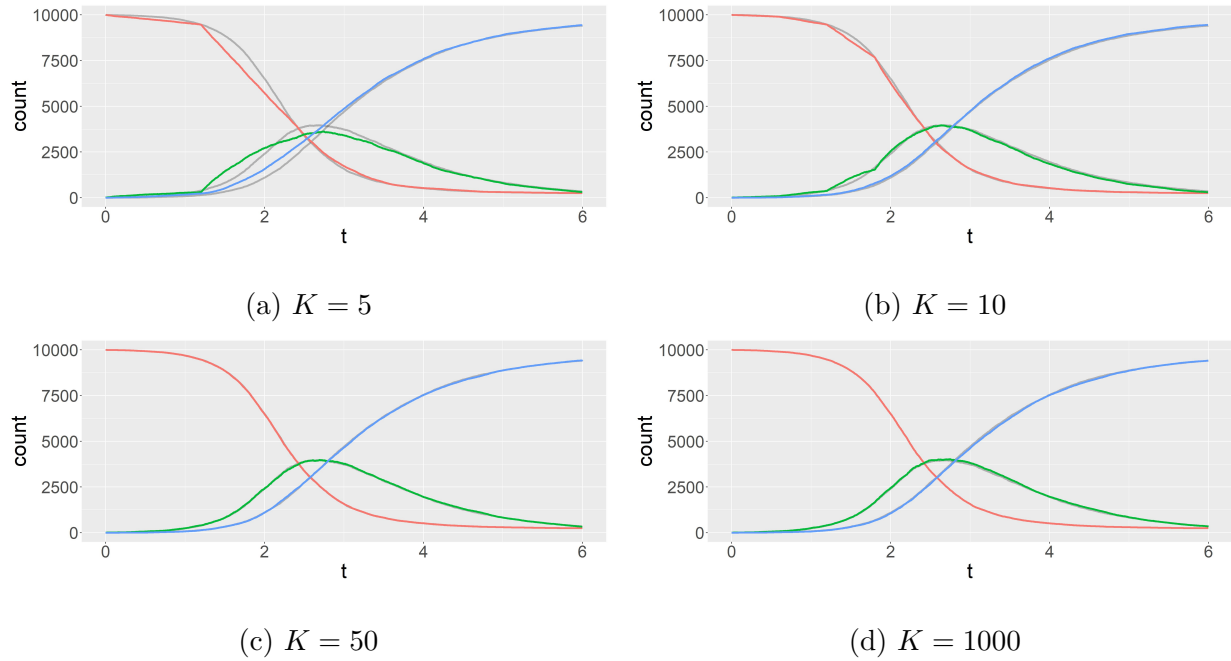


Figure 2: Compartment trajectories in a SIR (in colors, with S in red, I in green and R in blue) and a PD-SIR process (in grey) with the same infection incidence data $I_{1:K}$.

3.3 Uniform Ergodicity

We now turn to analyze the convergence properties of the Markov chain $\{(\theta^{(m)}, \mathbf{z}^{(m)})\}_m$ underlying the proposed MCMC algorithm. By construction, the joint posterior distribution $\pi(\theta, \mathbf{z}|\mathbf{Y})$ is invariant for the Gibbs kernel P_θ that updates θ and for the MH kernel $P_{\mathbf{z}}$ updating \mathbf{z} , and is therefore also invariant for the composite kernel $P = P_\theta P_{\mathbf{z}}$ of the MCMC algorithm (25). Moreover, P is strictly positive, implying that the chain is aperiodic and π -irreducible. Together with the existence of an invariant distribution, π -irreducibility implies that the chain is positive Harris recurrent and converges to $\pi(\theta, \mathbf{z}|\mathbf{Y})$. Hence, for any π -integrable function g , the ergodic theorem holds and the estimator

$$\bar{g}_m := \frac{1}{m} \sum_{i=0}^{m-1} g(\theta^{(m)}, \mathbf{z}^{(m)})$$

is consistent for $E_\pi g$, for any starting value.

A Markov chain is said to be *uniformly ergodic* if for some finite M and positive constant $r < 1$, the n -step transition kernel P^n satisfies

$$\|P^n(x, \cdot) - \pi(\cdot)\|_{TV} \leq Mr^n, \quad \forall x \in \chi$$

where $\|\mu\|_{TV} := \sup_A \mu(A)$ denotes the total variation norm of a signed measure μ . (?) shows that uniform ergodicity ensures the existence of a Central Limit Theorem for \bar{g}_m whenever $E_\pi|g|^2 < \infty$. That is,

$$\sqrt{m}(\bar{g}_m - E_\pi g) \Rightarrow N(0, \sigma_g^2)$$

for any initial distribution and for some positive, finite σ_g^2 . The constant σ_g^2 can be estimated via regeneration sampling, batch means or a spectral variance analysis (see (?)).

Toward establishing the uniform ergodicity of our DA-MCMC algorithm, we will show that the state space $\chi = \chi_\theta \times \chi_z$ of the Markov chain $\{(\theta^{(m)}, z^{(m)})\}_m$ is a *small set* for the transition kernel P ; that is, there exists a probability measure ν on the σ -algebra $\sigma(\chi)$ such that

$$P^m(x, \cdot) \geq \epsilon \nu(\cdot), \quad \forall x \in \chi \tag{15}$$

for a positive integer m and constant $\epsilon > 0$, which holds if and only if the Markov chain is uniformly ergodic (25). Theorem 3.2 shows that (15) holds for $m = 1$ for our MCMC algorithm when $\rho = 1$. This result is worth noting since the requirement that the whole space be small is extremely restrictive and is typically not satisfied for models with unbounded spaces.

Theorem 3.2. *For $\rho = 1$, the transition kernel P of the proposed DA-MCMC algorithm satisfies Equation (15) with $m = 1$, that is,*

$$P((\theta, z), \cdot) \geq \beta \nu(\cdot), \quad \forall (\theta, z) \in \chi_\theta \times \chi_z$$

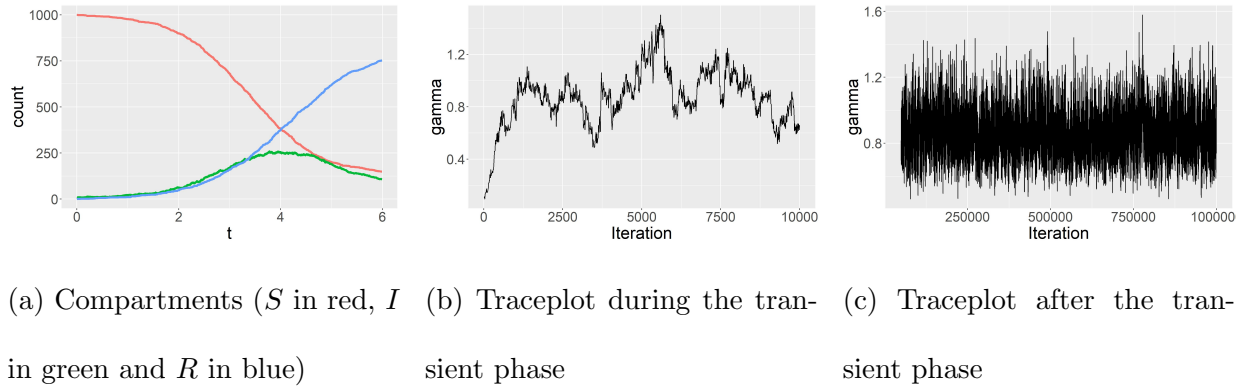
for some $\beta > 0$ and probability measure ν . As a result P is uniformly ergodic.

We provide a brief overview of the proof of Theorem 3.2, with details provided in Appendix B. Since the kernel $P = P_\theta P_{\mathbf{z}}$ is composite, it suffices to minorize $P_{\mathbf{z}}$ and P_θ separately. The density of the Gibbs kernel $P_{\mathbf{z}}$ corresponds to the product of the two gamma densities in (7); since the sufficient statistics of the latent data are bounded, these gamma densities possess a positive minorization whose closed form is derived in Appendix B. Furthermore, the MH kernel $P_{\mathbf{z}}$ depends on the current latent data only through the ratio $q(\mathbf{z}|\theta)/\pi(\mathbf{z}|\theta)$ which can be bounded above and away from zero. Finally, it is easy to see that, if $\rho < 1$, Equation (15) holds taking $m = \lfloor \rho^{-1} \rfloor$ for some ϵ and ν .

4 Performance on simulated and real epidemic data

4.1 Simulation Study

We validate the convergence properties of the proposed DA-MCMC empirically via a suite of simulation studies. First, we assess the performance of the algorithm in a moderately sized population of 1000 individuals. We simulate an epidemic with true parameters $(\beta, \gamma) = (0.0025, 1)$ — giving $R_0 = 2.5$ — starting with $(S(0), I(0)) = (1000, 10)$ until time $t_{end} = 6$, when the outbreak has completed most of its course but is not over yet, as depicted in Figure 3a where $I(t_{end}) = 122$. The numbers of infections in $K = 10$ equal-length time intervals are observed, corresponding to $I_{1:K} = (9, 14, 21, 42, 56, 121, 190, 162, 107, 73)$. We employ the parameterization $\tilde{\theta} = (\beta, R_0)$ and use the semi-conjugate prior distributions (9) with weakly informative hyperparameters $\beta \sim Ga(0.001, 1)$ and $R_0 \sim IG(1, 1)$. To evaluate the convergence speed of the Markov chain, we initialize it in a low density region at $(\beta^{(0)}, \gamma^{(0)}) = (\beta/10, \gamma/10)$. We keep every tenth draw for storage reasons and set $\rho = 0.2$, updating the trajectories of $\lceil \rho n \rceil = 202$ individuals in each MH step.



(a) Compartments (S in red, I in green and R in blue) (b) Traceplot during the transient phase (c) Traceplot after the transient phase

Figure 3: Performance of DA-MCMC in a medium-sized population for the parameter γ .

Remarkably, the algorithm takes less than 30 minutes to run 1 million iterations on a personal laptop. Figure 3b shows the traceplot of the parameter γ for the first 10000 iterations. We observe that the Markov chain quickly migrates from the low density region where it is initialized to the mode of the target distribution. The traceplot of γ after a burn-in period of 10000 iterations in Figure 3c indicates that once the chain reaches the high density region it mixes well. The acceptance rate of the MH step is 0.21. The posterior means of β , γ and R_0 are respectively 0.00217, 0.815 and 2.75, respectively based on 398, 370 and 438 effective sample sizes. The 90% equal-tailed Bayesian credible intervals are (0.00166, 0.00278), (0.492, 1.19) and (2.26, 3.45) and cover the true values of the parameters.

We now validate the estimation and uncertainty quantification of the posteriors under our algorithm over repeated simulations. To this end, we examine the frequentist coverage properties of the 90% equal-tailed Bayesian credible interval (BCI). We repeat the previous simulation 2000 times and compute the posterior mean of the parameters and the corresponding credible intervals. Since the prior is only weakly informative, the observed coverage rate of the BCI should be close to 90%. Table 1 provides the empirical coverage rate of the BCIs for the parameters β , γ and R_0 along with the average and variance of

Table 1: Empirical coverage of 90% posterior credible intervals and summary statistics of posterior means across 2000 independent runs in a medium-sized population, $n = 1000$. The true values of the parameters are $(\beta, \gamma, R_0) = (0.0025, 1, 2.5)$.

Parameter	Observed	Average of the	SD of the
	coverage rate	posterior means	posterior means
β	0.895	0.0025	0.000255
γ	0.902	1.00	0.142
R_0	0.910	2.54	0.194

the posterior means. As expected, the credible intervals cover the true values around 90% of the time, well within Monte Carlo error of the nominal coverage under a weakly informative prior. This result suggests that running the Markov chain for 1 million iterations is sufficient to approximate the posterior distribution of the parameters.

Second, we explore the impact of the tuning parameter ρ on the mixing properties of the algorithm as the population size varies. We simulate three realizations from the SIR process with $S(0) \in \{250, 500, 1000\}$ with $I(0) = 10$, $\gamma = 1$, $t_{end} = 6$ and $K = 10$ for each simulation. We choose β so that $R_0 \in \{3, 2.5, 2\}$ respectively, in order to have epidemics with comparable dynamics. For each population size and each value $\rho \in \{0.02, 0.05, 0.1, 0.25, 0.5, 1\}$, the DA-MCMC algorithm is run for 1 million iterations. We use the effective sample size per second to compare the resulting Markov chains.

Figures 4a and 4b show the run time of the algorithm and the acceptance rate in the MH step. We observe that, as expected, the run time increases with the population size and with ρ , which reflects the fact that the number of random variables to generate per

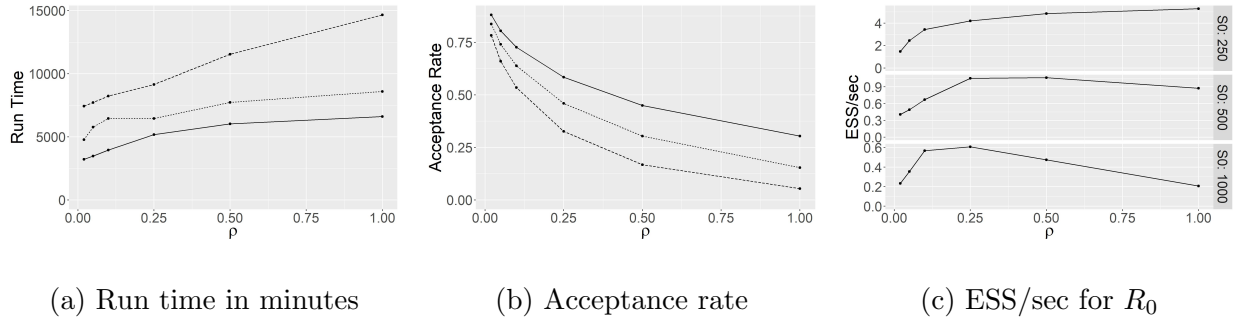


Figure 4: Impact of ρ on the performance of the DA-MCMC in a population of size 250 (solid), 500 (dotted) and 1000 (dashed).

iteration is proportional to $\lceil \rho n \rceil$. Moreover, the acceptance rate decreases as the number of trajectories updated per iteration $\lceil \rho n \rceil$ increases. Finally, the effect of ρ on the mixing properties of the Markov chain is presented in Figure 4c. We observe that for a population of 250 individuals updating the entire latent data in the MH step provides the best mixing; as the population size increases, however, the optimal value of ρ decreases. For instance, this suggests that, for a population of 1000 individuals, updating the whole latent data results in an excessively low acceptance rate, while updating less than 10% makes the updates too small to efficiently explore the latent space.

Finally, we showcase the efficacy of our joint proposal scheme through a comparison to a SSU DA-MCMC that is similar in spirit to those in (8), (20) and (5). We do not consider the particle filters of (16) nor the diffusion approximations of (6) since these methods are not suited to situations in which counts are observed without noise; see (11). The SSU sampler that we consider here is a special case of our DA-MCMC in which $\rho = (S(0) + I(0))^{-1}$, so that the infection and removal times of a single individual are updated per iteration. The two algorithms are run on the same data of a moderately sized population for 1 million iterations. Figure 5 presents the traceplots for γ as well as the auto-correlation function.

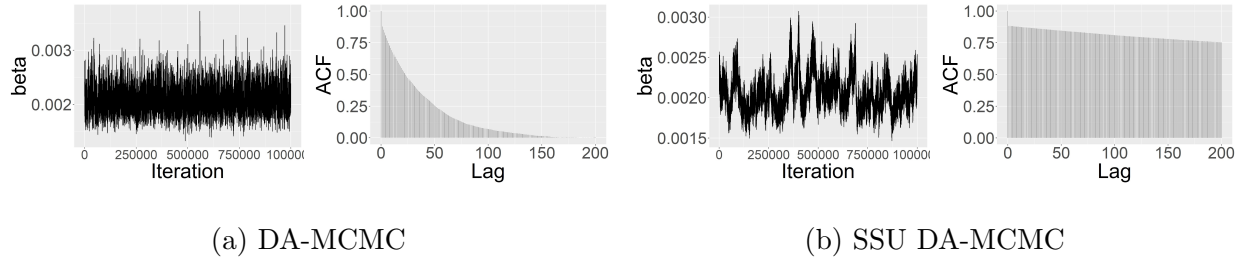


Figure 5: Traceplots and auto-correlation functions of the proposed DA-MCMC and the SSU DA-MCMC for β .

Table 2: Effective sample size per second for the proposed DA-MCMC and the single site update (SSU) DA-MCMC.

Parameter	DA-MCMC	SSU DA-MCMC
β	0.20	0.01
γ	0.19	0.01
R_0	0.38	0.05

We observe that the Markov chain mixes much better when event times are jointly proposed in the MH step. This is supported quantitatively in Table 2 which shows that the ESS per second obtained with the proposed DA-MCMC is between 7 and 20 times larger than that of the SSU DA-MCMC. Hence, even though the computation cost per iteration is larger for our algorithm, it mixes better than SSU algorithms and is more efficient overall.

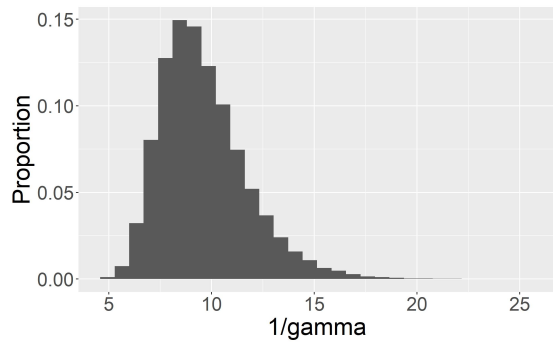
4.2 Ebola Outbreak in Guéckédou, Guinea

We now turn to a case study concerning the 2013-2015 Ebola outbreak in Western Africa. Between late 2013 and 2015, Guinea, along with several neighboring countries, experienced

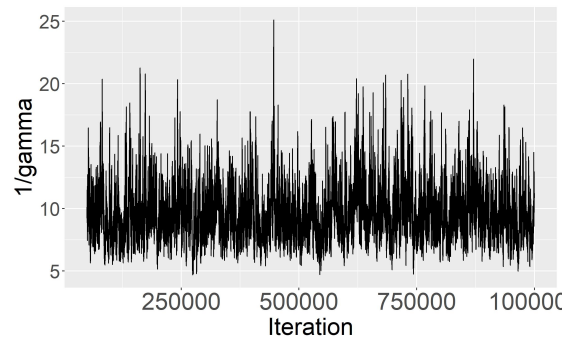
the largest outbreak of the Ebola virus disease in history. The virus, which has a fatality rate of 70%, was responsible for the death of almost 2000 people in Guinea alone. (?) traced back the origin of the outbreak to the Guéckédou prefecture of Guinea at the end of November 2013. Weekly infection incidence counts are available for each prefecture for the 73 weeks between the end of December 2013 and May 2015.

We fit the stochastic SIR model to these incidence counts for the Guéckédou prefecture using the DA-MCMC algorithm proposed in this article. It must be pointed that our model is illustrative and serves to show that fast and exact Bayesian inference can be made in a large population with the proposed algorithm rather than providing new insights into this outbreak or the Ebola virus in general. We assume that the population of the prefecture is closed and set the population size to $n = 292000$, the estimated number of people living in the Guéckédou prefecture in 2014. The units of time correspond to “days” in the analysis and $t = 0$ corresponds to Monday December 30, 2013, the first day of the observation period. As the first documented infection occurred late November (?), one month before the first reported incidence count, we set $I(0) = 5$.

The Markov chain is run for 1 million iterations and the event times of $\rho = 10\%$ of the individuals are updated each iteration. The initial values of the parameters are set to $(\beta^{(0)}, \gamma^{(0)}) = (10^{-7}, 0.05)$ and we use the parameterization $\tilde{\theta} = (\beta, R_0)$ with the weakly informative semi-conjugate prior distributions $\beta \sim Ga(0.001, 1)$ and $R_0 \sim IG(1, 1)$. Even for such a large population, the total run time of the algorithm was less than 50 minutes on a personal laptop. The Metropolis-Hastings step for the latent data proposals achieves a healthy 20.1% acceptance rate, and the first 50,000 iterations of the Markov chain are discarded as a burn-in. Figure 6 shows the marginal posterior distributions γ^{-1} which indicates that people remained infectious for around 9 days on average, which is consistent



(a) Posterior distribution



(b) Traceplot

Figure 6: Posterior distribution and traceplot of the expected infection length (γ^{-1}) for the Guéckédou prefecture.

with the existing literature.

5 Discussion and Conclusion

The proposed method enables the classical Metropolis-Hastings algorithm to be an efficient way to conduct exact posterior inference under the stochastic SIR model, given only incidence data for infections. In contrast to methods that rely on approximate computation of simplifying assumptions necessitated by computational considerations such as (17) and (6), our data-augmented algorithm enables exact and fast Bayesian inference, even for large outbreaks, and leverages a well-studied, transparent MCMC framework with guarantees of uniform ergodicity.

Central to the success of the DA-MCMC algorithm is an efficient proposal scheme for the latent variables that swiftly explores the latent space of epidemic paths that are compatible with the observed data. The PD-SIR process possesses three features that make it such an efficient proposal in our DA-MCMC. First, generating a PD-SIR process is extremely fast;

it only requires the simulation of truncated exponential distributions, which can efficiently be realized via the inverse cumulative distribution function method. Moreover, the piecewise constant infection rate of the PD-SIR is only updated K times, as opposed to after each event in the SIR model. Second, generating a PD-SIR process that is constrained to be compatible with the observed incidence data can be done at no additional cost; in contrast, directly generating a SIR process compatible with the observed data would be prohibitively slow (13). Third, the dynamics of the PD-SIR process closely resemble those of the SIR process: the removal dynamics are identical and, for short observation time intervals, the infection dynamics are also very similar in the two processes.

The first two features make the algorithm extremely fast and scalable for populations with hundreds of thousands of individuals. Because the PD-SIR process enables the algorithm to update a large portion of the augmented data in each iteration while maintaining a healthy acceptance rate. As a result, the Markov chain makes large jumps in the latent space and has very good mixing properties. In contrast, existing DA-MCMC algorithms (8; 20; 5) keep most of the latent space fixed across iterations and their Markov chains and therefore mix much more slowly.

Our algorithm features a tuning parameter ρ that determines the proportion of individuals whose trajectory is updated per iteration, which in turn affects the acceptance ratio. Larger values for ρ enable the chain to make larger steps in the latent space but may result in an excessively low acceptance rate, while smaller values of ρ result in a higher acceptance rate but constrain the chain to make small jumps. Depending on the size of the population, different values of the tuning parameter are optimal, and future work may seek theoretical insights to this end. To find a value that optimizes the mixing properties of the chain in practice, one can use several short runs of the algorithm with different values for ρ and

select the value that yields the largest effective size per second.

The DA-MCMC algorithm proposed in this article is specific to the stochastic SIR model. However, one can argue that it is a simplistic representation of the spread of disease, relying on assumptions such as perfect reporting, exponentially-distributed infectious periods, homogeneously mixing population and a constant infection rate. Our data-augmentation framework and the idea of a faithful surrogate proposal can be extended to models of increasing realism where these assumptions are relaxed. It will be fruitful to consider extensions to epidemic models accounting for under-reporting (5?), non-Markovian dynamics (?), non-homogeneous mixing (22?) as well as time-varying infection rates (?) in future work. We invite readers to consider applications of these ideas in other stochastic process models with complex latent spaces that may similarly be made navigable through designing tractable, mechanistic proposal processes.

Appendix

A Proof of Theorem 3.1

Theorem 3.1 was first proved by (19). (?) provide a simpler proof which we now give.

Proof. Consider a linear pure death process with n particles and individual death rate μ . Let T_i be the time of the i th death. Then $W_1 = T_1 \sim \text{Exp}(n\mu)$ and $W_i = T_i - T_{i-1} \sim$

$\text{Exp}((n-i)\mu)$ independently. Let N be the number of deaths by time t . Then,

$$\begin{aligned}
& f(T_1 = t_1, \dots, T_N = t_N | N) \\
& \propto f(T_1 = t_1, \dots, T_N = t_N, T_{N+1} > t) \mathbf{1}\{t_N < t\} \\
& \propto f(W_1 = t_1, W_2 = t_2 - t_1, \dots, W_N = t_N - t_{N-1}, W_{N+1} > t - t_N) \mathbf{1}\{t_N < t\} \\
& \propto \exp\{-n\mu t_1\} \exp\{-(n-1)\mu(t_2 - t_1)\} \dots \exp\{-(n-N)\mu(t - t_N)\} \mathbf{1}\{t_N < t\} \\
& \propto \exp\{-\mu t_1\} \exp\{-\mu t_2\} \dots \exp\{-\mu t_N\} \mathbf{1}\{t_N < t\}
\end{aligned}$$

which corresponds to the kernels of independent exponential distribution truncated above by t . By the memoryless property of the exponential distribution, this results can be extended from the interval $(0, t]$ to any interval.

□

B Proof of Theorem 3.2

We first present two lemmas that will be useful in the proof of Theorem 3.2.

Lemma B.1. *Let $Ga(x; a, b) = \frac{a^b}{\Gamma(a)} x^{a-1} \exp\{-ab\}$ denote the density of the gamma distribution with shape a and rate b evaluated at x . Then*

$$\inf_{0 \leq \beta \leq B} Ga(x; a, b + \beta) = \begin{cases} Ga(x; a, b), & x < x_a^* \\ Ga(x; a, b + B), & x \geq x_a^* \end{cases} \quad (16)$$

where $x_a^* = \frac{a}{B} \log(1 + \frac{B}{b})$. Moreover,

$$\inf_{0 \leq \alpha \leq A} Ga(x; a + \alpha, b) = \begin{cases} Ga(x; a, b), & x > x_b^* \\ Ga(x; a + A, b), & x \leq x_b^* \end{cases} \quad (17)$$

where $x_b^* = \frac{1}{b} \left[\frac{\Gamma(a+A)}{\Gamma(a)} \right]^{1/A}$.

Proof. Equation (16) is proven in (?). For Equation (17), note that x_b^* is the only positive solution to $Ga(x; a, b) = Ga(x; a + A, b)$. Now, for all $0 < x \leq x_b^*$ and all $0 \leq \alpha \leq A$, we have

$$\begin{aligned}
\frac{Ga(x; a + A, b)}{Ga(x; a + \alpha, b)} &= b^{A-\alpha} x^{A-\alpha} \frac{\Gamma(a + \alpha)}{\Gamma(a + A)} \\
&\leq b^{A-\alpha} \left(\frac{1}{b} \left[\frac{\Gamma(a + A)}{\Gamma(a)} \right]^{1/A} \right)^{A-\alpha} \frac{\Gamma(a + \alpha)}{\Gamma(a + A)} \\
&= \left[\frac{\Gamma(a + A)}{\Gamma(a)} \right]^{(A-\alpha)/A} \frac{\Gamma(a + \alpha)}{\Gamma(a + A)} \\
&= \left[\frac{\left(\frac{\Gamma(a+A)}{\Gamma(a)} \right)^{1/A}}{\left(\frac{\Gamma(a+A)}{\Gamma(a+\alpha)} \right)^{1/(A-\alpha)}} \right]^{A-\alpha} \\
&= \left(\frac{\Gamma_{a,a+A}}{\Gamma_{a+\alpha,a+A}} \right)^{A-\alpha} \\
&\leq 1,
\end{aligned}$$

where $\Gamma_{d,e} = \left(\frac{\Gamma(e)}{\Gamma(d)} \right)^{\frac{1}{e-d}}$ is a geometric mean, and where the last inequality holds because $\Gamma_{a,a+A} \leq \Gamma_{a+\alpha,a+A}$. The case $x > x_b^*$ is analogous and is omitted for brevity. \square

Figures 7a and 7b illustrate these two results. Lemma B.1 can be used to obtain a closed form solution to the minimization of a gamma density of the form

$$Ga(x; a + \alpha, b + \beta) = \frac{(b + \beta)^{a+\alpha}}{\Gamma(a + \alpha)} x^{a+\alpha-1} \exp\{-x(b + \beta)\}, \quad 0 \leq \alpha \leq A, 0 \leq \beta \leq B. \quad (18)$$

jointly over α and β for each value of x . To this end, we establish the following technical lemma.

Lemma B.2. *For a fix $x > 0$, the density $Ga(x; a + \alpha, b + \beta)$ is minimized by $(\alpha, \beta) \in$*

$\{(A, 0), (0, B)\}$, the minimizing set of values depending on x . In particular,

$$\inf_{\substack{0 \leq \alpha \leq A \\ 0 \leq \beta \leq B}} Ga(x; a+\alpha, b+\beta) = \begin{cases} Ga(x; a+A, b), & x < x_a \text{ or } x < x_{a+A}^* \vee x_b^* \\ Ga(x; a, b+B), & x_{a+A}^* < x \text{ or } x_a^* \wedge x_{b+B}^* < x \\ \min\{Ga(x; a+A, b), Ga(x; a, b+B)\}, & x_a^* \wedge x_b^* \leq x < x_{a+A}^* \vee x_{b+B}^* \end{cases}$$

Proof. Given $x > 0$, (16) shows that for a fixed α , the gamma density (18) is minimized by $\beta \in \{0, B\}$. Similarly, (17) shows that for a fixed β , $\alpha \in \{0, A\}$ minimizes (18). This implies that for a fixed $x > 0$, the gamma density (18) is minimized by $(\alpha, \beta) \in \{(0, 0), (A, 0), (0, B), (A, B)\}$.

A case-by-case analysis of the nine possibilities

$$(x < x_a^*; x_a^* < x < x_{a+A}^*; x_{a+A}^* < x) \times (x < x_{b+B}^*; x_{b+B}^* < x < x_b^*; x_b^* < x)$$

is presented in Table 3 and shows that it is sufficient to consider $(\alpha, \beta) \in \{(A, 0), (0, B)\}$.

Table 3: Values of (α, β) that minimize $Ga(x; a + \alpha, b + \beta)$ for different values x .

	$x < x_a^*$	$x_a^* \leq x < x_{a+A}^*$	$x_{a+A}^* < x$
$x < x_b^*$	$(a + A, b)$	$(a + A, b)$	
$x_b^* \leq x < x_{b+B}^*$	$(a + A, b)$	ad hoc	$(a, b + B)$
$x_{b+B}^* < x$		$(a, b + B)$	$(a, b + B)$

The two empty entries in Table 3 correspond to configurations that are impossible.

Indeed, we must have $x_b^* > x_a^*$ and $x_{a+A}^* > x_{b+B}^*$ for all a, A, b, B since

$$\frac{x_b^*}{x_a^*} = \frac{\left(\frac{\Gamma(a+A)}{\Gamma(a)}\right)^{1/A} b^{-1}}{a B^{-1} \log(1 + B/b)} = \frac{\left(\frac{\Gamma(a+A)}{\Gamma(a)}\right)^{1/A}}{a} \frac{B/b}{\log(1 + B/b)} = \frac{\Gamma_{a,a+A}}{a} \frac{B/b}{\log(1 + B/b)} \geq 1$$

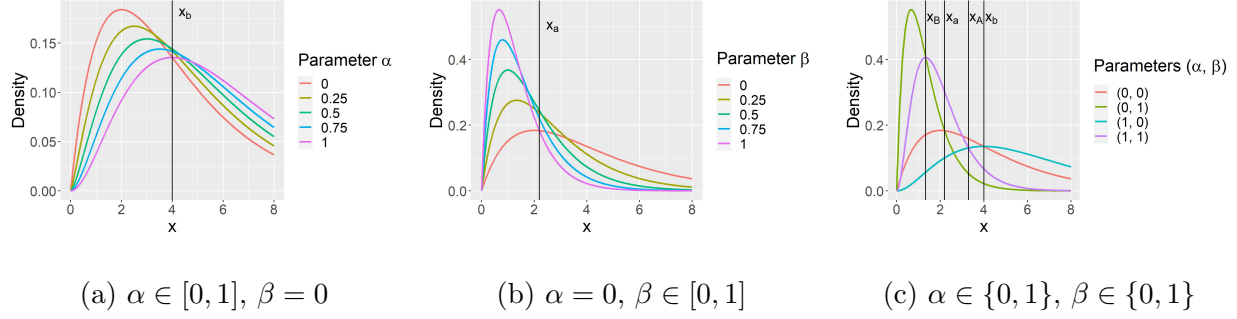


Figure 7: Example of minorization of the density of a gamma distribution $Ga(2+\alpha, 0.5+\beta)$.

where the inequality hold since $a \leq \Gamma_{a,a+A}$ and $\frac{y}{\log(1+y)} \geq 1$, and

$$\frac{x_{b+B}^*}{x_{a+A}^*} = \frac{\left(\frac{\Gamma(a+A)}{\Gamma(a)}\right)^{1/A} (b+B)^{-1}}{(a+A)B^{-1} \log(1+B/b)} = \frac{\Gamma_{a,a+A}}{a+A} \frac{B}{b+B} \frac{1}{\log(1+B/b)} \leq 1$$

where the inequality holds since $\Gamma_{a,a+A} \leq a+A$.

If $x_a^* \wedge x_{b+B}^* \leq x < x_{a+A}^* \vee x_b^*$, which corresponds to the middle entry of the center column in Table 3, then one needs to directly check which set of values in $\{(0, 0), (A, 0), (0, B), (A, B)\}$ minimizes (18). In fact, it is sufficient to consider only $\{(A, 0), (0, B)\}$ since

$$Ga(x, a+A, b) \leq \begin{cases} Ga(x; a, b), & x < x_b^* \\ Ga(x; a+A, b+B), & x < x_{a+A}^* \end{cases}$$

and

$$Ga(x, a, b+B) \leq \begin{cases} Ga(x; a, b), & x > x_a^* \\ Ga(x; a+A, b+B), & x > x_{b+B}^* \end{cases}$$

□

We can now proceed with the proof of Theorem 3.2.

Proof. The transition kernel $P = P_\theta P_{\mathbf{z}}$ is a composition of two kernels. The kernel P_θ updates the parameters θ while keeping the latent data \mathbf{z} fixed, and $P_{\mathbf{z}}$ update \mathbf{z} while keeping θ fixed. We therefore have

$$P((\theta_1, \mathbf{z}_1), (d\theta_2, d\mathbf{z}_2)) = P_\theta(\theta_1, d\theta_2 | \mathbf{z}_1) P_{\mathbf{z}}(\mathbf{z}_1, d\mathbf{z}_2 | \theta_2)$$

where

$$\begin{aligned} P_\theta(\theta_1, d\theta_2 | \mathbf{z}_1) &= \pi(d\theta_2 | \mathbf{z}_1) \\ &= \pi(\beta_2 | \mathbf{z}_1) \pi(\gamma_2 | \mathbf{z}_1) d\beta_2 d\gamma_2 \end{aligned} \tag{19}$$

corresponds to the transition kernel of a Gibbs sampler and

$$\begin{aligned} P_{\mathbf{z}}(\mathbf{z}_1, d\mathbf{z}_2 | \theta_2) &= Q(d\mathbf{z}_2 | \theta_2) \alpha((\theta_2, \mathbf{z}_1), (\theta_2, \mathbf{z}_2)) + \delta_{\mathbf{z}_1}(d\mathbf{z}_2) \int (1 - \alpha((\theta_2, \mathbf{z}_1), (\theta_2, \mathbf{z}_2))) Q(d\mathbf{z}_2 | \theta_2) \\ &\geq Q(d\mathbf{z}_2 | \theta_2) \alpha((\theta_2, \mathbf{z}_1), (\theta_2, \mathbf{z}_2)) \\ &= q(\mathbf{z}_2 | \theta_2) \min \left\{ 1, \frac{\pi(\theta_2, \mathbf{z}_2) q(\mathbf{z}_1 | \theta_2)}{\pi(\theta_2, \mathbf{z}_1) q(\mathbf{z}_2 | \theta_2)} \right\} d\mathbf{z}_2 \end{aligned} \tag{20}$$

corresponds to a Metropolis-Hastings transition kernel in which a new configuration of the latent data is generated from the proposal kernel Q conditionally on the current value of the parameters θ_2 , but independently of the current configuration \mathbf{z}_1 . The density q of the proposal kernel Q is given in (14).

To show that χ is a small state, it suffices to show that there exists a positive function k such that

$$k(\theta_2, \mathbf{z}_2) \leq \pi(\beta_2 | \mathbf{z}_1) \pi(\gamma_2 | \mathbf{z}_1) q(\mathbf{z}_2; \theta_2) \min \left\{ 1, \frac{\pi(\theta_2, \mathbf{z}_2) q(\mathbf{z}_1 | \theta_2)}{\pi(\theta_2, \mathbf{z}_1) q(\mathbf{z}_2 | \theta_2)} \right\} \tag{21}$$

for all $\theta_1 \in \chi_\theta$ and all $\mathbf{z}_1 \in \chi_{\mathbf{z}}$. Indeed, suppose that we can find a positive function k satisfying the inequality (21), then for any set A and any (θ, \mathbf{z}) we have, by (19), (20) and

(21),

$$\begin{aligned}
P((\theta, \mathbf{z}), A) &\geq \int_A \pi(\theta'|\mathbf{z})\pi(\beta'|\mathbf{z})\pi(\gamma'|\mathbf{z}) \min \left\{ 1, \frac{\pi(\theta', \mathbf{z}')q(\mathbf{z}|\theta')}{\pi(\theta', \mathbf{z})q(\mathbf{z}'|\theta')} \right\} d(\beta', \gamma', \mathbf{z}') \\
&\geq \int_A k(\theta', \mathbf{z}')d(\theta', \mathbf{z}') \\
&= \epsilon\nu(A)
\end{aligned}$$

with $\epsilon = \int k(\theta, \mathbf{z})d(\theta, \mathbf{z})$ a positive constant and $\nu(A) = \epsilon^{-1} \int_A k(\theta, \mathbf{z})d(\theta, \mathbf{z})$ a probability measure.

We now construct a positive function k satisfying (21). The inequality depends on (θ_1, \mathbf{z}_1) only through the full conditional distributions $\pi(\beta_2|\mathbf{z}_1)$ and $\pi(\gamma_2|\mathbf{z}_1)$ and the ratio $\frac{q(\mathbf{z}_1|\theta_2)}{\pi(\theta_2, \mathbf{z}_1)}$. It therefore suffices to find positive functions k_β, k_γ and k_r such that, for all \mathbf{z}_1 ,

$$k_\beta(\beta_2) \leq \pi(\beta_2|\mathbf{z}_1), \quad k_\gamma(\gamma_2) \leq \pi(\gamma_2|\mathbf{z}_1), \quad \text{and} \quad k_r(\theta_2) \leq \frac{q(\mathbf{z}_1|\theta_2)}{\pi(\theta_2, \mathbf{z}_1)}.$$

First, we obtain a closed form minorization of $\pi(\beta_2|\mathbf{z}_1)$ using Proposition B.1 as follows,

$$\begin{aligned}
\pi(\beta_2|\mathbf{z}_1) &= Ga \left(\beta_2; a_\beta + n_I, b_\beta + \int_0^{t_{end}} S(t)I(t)dt \right) \\
&\geq \inf_{0 \leq \int_0^{t_{end}} S(t)I(t)dt \leq n(n_I + I_0)t_{end}} Ga \left(\beta_2; a_\beta + n_I, b_\beta + \int_0^{t_{end}} S(t)I(t)dt \right) \\
&= \min \{ Ga(\beta_2; a_\beta + n_I, b_\beta), Ga(\beta_2; a_\beta + n_I, b_\beta + n(n_I + I_0)t_{end}) \} \\
&= k_\beta(\beta_2) > 0
\end{aligned}$$

since $n_I = \sum_k I_k$ is known and the sufficient statistic from \mathbf{z}_1 , $\int_0^{t_{end}} S(t)I(t)dt$, is bounded

between 0 and $n(n_I + I_0)t_{end}$. Similarly, by Proposition B.2, we minorize $\pi(\gamma_2|\mathbf{z}_1)$ as follows,

$$\begin{aligned}
\pi(\gamma_2|\mathbf{z}_1) &= Ga\left(\gamma_2; a_\beta + n_R, b_\beta + \int_0^{t_{end}} I(t)dt\right) \\
&\geq \inf_{\substack{0 \leq n_R \leq n_I + I_0, \\ 0 \leq \int_0^{t_{end}} I(t)dt \leq (n_I + I_0)t_{end}}} Ga\left(\gamma_2; a_\beta + n_R, b_\beta + \int_0^{t_{end}} I(t)dt\right) \\
&= \min\{Ga(\gamma_2; a_\gamma + n_R + I_0, b_\gamma), Ga(\gamma_2; a_\gamma, b_\gamma + (n_I + I_0)t_{end})\} \\
&= k_\gamma(\gamma_2) > 0
\end{aligned}$$

since the sufficient statistics from \mathbf{z}_1 , n_R and $\int_0^{t_{end}} I(t)dt$, are respectively bounded between 0 and $n_I + I_0$, and between 0 and $(n_I + I_0)t_{end}$.

Finally, the ratio $\frac{q(\mathbf{z}_1|\theta_2)}{\pi(\theta_2, \mathbf{z}_1)}$ can be minorized as follows,

$$\begin{aligned}
\frac{q(\mathbf{z}_1|\theta_2)}{\pi(\theta_2, \mathbf{z}_1)} &= \frac{\prod_{k=1}^K \prod_{j \in \mathcal{I}_k} \text{TrunExp}(z_j^I; \mu_k, t_{k-1}, t_k) \prod_{i=1}^n (1-p_i)^{1\{z_i^R=\infty\}} (p_i \text{TrunExp}(z_i^R; \gamma, z_i^I, t_{end}))^{1\{z_i^R \leq t_{end}\}}}{\beta^{n_I} \prod_{l \in \mathcal{I}} I(z_l^I) \gamma^{n_R} \exp\{-\beta \int_0^{t_{end}} S(t)I(t)dt - \gamma \int_0^{t_{end}} I(t)dt\}} \\
&= \frac{\prod_{k=1}^K \prod_{j \in \mathcal{I}_k} \text{TrunExp}(z_j^I; \mu_k, t_{k-1}, t_k)}{\prod_{l \in \mathcal{I}} \beta I(z_l^I) \exp\{-\beta \int_0^{t_{end}} S(t)I(t)dt\}} \\
&= \frac{\prod_{k=1}^K \prod_{j \in \mathcal{I}_k} \frac{\beta I(t_{k-1}) \exp\{-\beta I(t_{k-1})(z_j^I - t_{k-1})\}}{1 - \exp\{-\beta I(t_{k-1})(t_k - t_{k-1})\}}}{\prod_{l \in \mathcal{I}} \beta I(z_l^I) \exp\{-\beta \int_0^{t_{end}} S(t)I(t)dt\}} \\
&\geq \frac{\prod_{k=1}^K \prod_{j \in \mathcal{I}_k} I(t_{k-1}) \exp\{-\beta I(t_{k-1})(z_j^I - t_{k-1})\}}{\prod_{l \in \mathcal{I}} I(z_l^I) \exp\{-\beta \int_0^{t_{end}} S(t)I(t)dt\}} \\
&\geq \frac{\prod_{k=1}^K \prod_{j \in \mathcal{I}_k} \exp\{-\beta n(t_k - t_{k-1})\}}{n^{n_I}} \\
&= k_r(\beta_2),
\end{aligned}$$

where the second equality holds since the contribution of the removal times in the numerator and the denominator cancel each other as the removal times are generated from the same

distribution under the SIR and the PD-SIR processes:

$$\begin{aligned}
& \frac{\prod_{i=1}^n (1-p_i)^{\mathbf{1}\{z_i^R=\infty\}} (p_i \text{TrunExp}(z_i^R; \gamma, z_i^I, t_{end}))^{\mathbf{1}\{z_i^R \leq t_{end}\}}}{\gamma^{n_R} \exp\{-\gamma \int_0^{t_{end}} I(t) dt\}} \\
&= \frac{\prod_{j \in \mathcal{R}^c} \exp\{-\gamma(t_{end} - z_j^I)\} \prod_{k \in \mathcal{R}} (1 - \exp\{\gamma(t_{end} - z_k^I)\}) \frac{\gamma \exp\{-\gamma(z_k^R - z_k^I)\}}{1 - \exp\{\gamma(t_{end} - z_k^I)\}}}{\gamma^{n_R} \exp\{\gamma \sum_{i=1}^n \min\{z_i^R, t_{end}\} - z_i^I\}} \\
&= \frac{\exp\{-\gamma \sum_{j \in \mathcal{R}^c} (t_{end} - z_j^I)\} \gamma^{n_R} \exp\{-\gamma \sum_{k \in \mathcal{R}} (z_k^R - z_k^I)\}}{\gamma^{n_R} \exp\{-\gamma [\sum_{j \in \mathcal{R}^c} (t_{end} - z_j^I) + \sum_{k \in \mathcal{R}} (z_k^R - z_k^I)]\}} \\
&= 1,
\end{aligned}$$

the first inequality holds because $1 - \exp\{-\beta I(t_{k-1})(t_k - t_{k-1})\} \leq 1$ and the second inequality holds because $1 \leq I(\cdot) \leq n$, $0 \leq \int_0^{t_{end}} S(t) I(t) dt$ and $z_j^I \leq t_k$ when $j \in \mathcal{I}_k$.

Taken together, these inequalities give

$$\begin{aligned}
& \pi(\beta_2 | \mathbf{z}_1) \pi(\gamma_2 | \mathbf{z}_1) q(\mathbf{z}_2; \theta_2) \min \left\{ 1, \frac{\pi(\theta_2, \mathbf{z}_2) q(\mathbf{z}_1 | \theta_2)}{\pi(\theta_2, \mathbf{z}_1) q(\mathbf{z}_2 | \theta_2)} \right\} \geq k_\beta(\beta_2) k_\gamma(\gamma_2) q(\mathbf{z}_2; \theta_2) \min \left\{ 1, k_r(\beta_2) \frac{\pi(\theta_2, \mathbf{z}_2)}{q(\mathbf{z}_2 | \theta_2)} \right\} \\
&= k(\theta_2, \mathbf{z}_2)
\end{aligned}$$

for all $\theta_1 \in \chi_\theta$ and all $\mathbf{z}_1 \in \chi_{\mathbf{z}}$, which completes the proof.

□

References

- [1] Helen Abbey. An examination of the reed-frost theory of epidemics. *Human biology*, 24(3):201, 1952.
- [2] Sylvain Baize, Delphine Pannetier, Lisa Oestereich, Toni Rieger, Lamine Koivogui, N’Faly Magassouba, Barrè Soropogui, Mamadou Saliou Sow, Sakoba Keita, Hilde de Clerck, et al. Emergence of zaire ebola virus disease in guinea. *New England Journal of Medicine*, 371(15):1418–1425, 2014.

- [3] Niels G. Becker. On a general stochastic epidemic model. *Theoretical Population Biology*, 11(1):23–36, 1977.
- [4] Simon Cauchemez and Neil M. Ferguson. Likelihood-based estimation of continuous-time epidemic models from time-series data: application to measles transmission in london. *Journal of the Royal Society Interface*, 5(25):885–897, 2008.
- [5] Jonathan Fintzi, Xiang Cui, Jon Wakefield, and Vladimir N. Minin. Efficient data augmentation for fitting stochastic epidemic models to prevalence data. *Journal of Computational and Graphical Statistics*, 26(4):918–929, 2017.
- [6] Jonathan Fintzi, Jon Wakefield, and Vladimir N. Minin. A linear noise approximation for stochastic epidemic models fit to partially observed incidence counts. *arXiv preprint arXiv:2001.05099*, 2020.
- [7] Alan E. Gelfand and Adrian F. M. Smith. Sampling-based approaches to calculating marginal densities. *Journal of the American statistical association*, 85(410):398–409, 1990.
- [8] Gavin J. Gibson and Eric Renshaw. Estimating parameters in stochastic compartmental models using markov chain methods. *Mathematical Medicine and Biology: A Journal of the IMA*, 15(1):19–40, 1998.
- [9] Peter J. Green. Reversible jump markov chain monte carlo computation and bayesian model determination. *Biometrika*, 82(4):711–732, 1995.
- [10] Major Greenwood. On the statistical measure of infectiousness. *Epidemiology & Infection*, 31(3):336–351, 1931.

- [11] Lam Si Tung Ho, Forrest W. Crawford, Marc A. Suchard, et al. Direct likelihood-based inference for discretely observed stochastic compartmental models of infectious disease. *The Annals of Applied Statistics*, 12(3):1993–2021, 2018.
- [12] Lam Si Tung Ho, Jason Xu, Forrest W. Crawford, Vladimir N. Minin, and Marc A. Suchard. Birth/birth-death processes and their computable transition probabilities with biological applications. *Journal of mathematical biology*, 76(4):911–944, 2018.
- [13] Asger Hobolth and Eric A. Stone. Simulation from endpoint-conditioned, continuous-time markov chains on a finite state space, with applications to molecular evolution. *The Annals of Applied Statistics*, 3(3):1204, 2009.
- [14] Roman Jandarov, Murali Haran, Ottar Bjørnstad, and Bryan Grenfell. Emulating a gravity model to infer the spatiotemporal dynamics of an infectious disease. *Journal of the Royal Statistical Society: Series C: Applied Statistics*, pages 423–444, 2014.
- [15] William Ogilvy Kermack and Anderson G. McKendrick. A contribution to the mathematical theory of epidemics. *Proceedings of the royal society of london. Series A, Containing papers of a mathematical and physical character*, 115(772):700–721, 1927.
- [16] Aaron A. King, Dao Nguyen, and Edward L. Ionides. Statistical inference for partially observed markov processes via the r package pomp. *arXiv preprint arXiv:1509.00503*, 2015.
- [17] Trevelyan J. McKinley, Ian Vernon, Ioannis Andrianakis, Nicky McCreesh, Jeremy E. Oakley, Rebecca N. Nsubuga, Michael Goldstein, Richard G. White, et al. Approximate bayesian computation and simulation-based inference for complex stochastic epidemic models. *Statistical science*, 33(1):4–18, 2018.

- [18] Peter Neal and Gareth Roberts. A case study in non-centering for data augmentation: stochastic epidemics. *Statistics and Computing*, 15(4):315–327, 2005.
- [19] Marcel F. Neuts and Sidney I. Resnick. On the times of births in a linear birthprocess. *Journal of the Australian Mathematical Society*, 12(4):473–475, 1971.
- [20] Philip D. O'Neill and Gareth O. Roberts. Bayesian inference for partially observed stochastic epidemics. *Journal of the Royal Statistical Society: Series A (Statistics in Society)*, 162(1):121–129, 1999.
- [21] C. M. Pooley, S. C. Bishop, and G. Marion. Using model-based proposals for fast parameter inference on discrete state space, continuous-time markov processes. *Journal of the Royal Society Interface*, 12(107):20150225, 2015.
- [22] Norman C. Severo. Generalizations of some stochastic epidemic models. *Mathematical biosciences*, 4(3-4):395–402, 1969.
- [23] Aidan Sudbury. The proportion of the population never hearing a rumour. *Journal of applied probability*, pages 443–446, 1985.
- [24] Martin A. Tanner and Wing Hung Wong. The calculation of posterior distributions by data augmentation. *Journal of the American statistical association*, 82(398):528–540, 1987.
- [25] Luke Tierney. Markov chains for exploring posterior distributions. *the Annals of Statistics*, pages 1701–1728, 1994.
- [26] Ray Watson. An application of a martingale central limit theorem to the standard epidemic model. *Stochastic Processes and Their Applications*, 11(1):79–89, 1981.